Transistor Distortion Analysis Using Volterra Series Representation

By S. NARAYANAN

(Manuscript received January 3, 1967)

Intermodulation distortion due to nonlinear elements in transistors is analyzed using Volterra series representation. It is shown that this technique is well suited for the analysis of transistor distortion where the nonlinearities are small but frequency dependent. An ac transistor model incorporating four nonlinearities is briefly described. The nonlinear nodal equations of the model are successively solved by expressing nodal voltages in terms of the Volterra series expansion of the input voltage. Based on this analysis, a digital computer program has been developed which computes the second and the third harmonic distortion for a given set of input frequencies and transistor parameters. The results compare favorably with measured values. This method also enables the derivation of closed form ac expressions for a simplified model; these expressions show the dependence of distortion on frequency, load and source impedances, bias currents and voltages, and the parameters of the transistor. The technique is also extended to cascaded transistors, and simplified expressions for the overall distortion in terms of the distortion and gain of individual transistors are derived. Finally, a few pertinent practical applications are discussed.

1. INTRODUCTION

Solid-state long-haul analog communication systems are being designed for higher frequencies to meet the growth in demand. One of the more critical and significant problems facing the system designer is intermodulation noise arising from transistor nonlinearities. Thus, an analysis of transistor distortion at higher frequencies is a practical problem; this paper investigates the transistor distortion using the Volterra series as an analysis tool.

Transistor distortion has been investigated in some detail previously. Many authors have considered the exponential nonlinear relation between emitter current and emitter-to-base voltage which is important

at low currents.[1,2,3,4,5] The effect of frequency on this nonlinear source alone has been reported.[5] Three nonlinearities (exponential, avalanche, and h_{FE} at dc) have been examined by Riva, Benetcau and Dallavolta.[6] For currents up to 20 mA and frequencies up to 100 kHz, Meyer[7,8,9] has developed a more accurate and complex model obtaining the nonlinearities from h-parameters. However, he takes into account the frequency dependence by assuming that the h-parameters can be written as $h' + j\omega h''$. Moreover, he does not take into account avalanche distortion, nor has he extended the model to higher currents (100 mA) and frequencies (20 MHz). The model described here considers four nonlinearities; they are, exponential, avalanche, h_{FE}, and collector capacitance nonlinearities. These nonlinearities are superimposed on a linear ac equivalent circuit.[10,11] Much of the initial development of the model with three nonlinearities was done by Thomas.[10]

The transistor model is analyzed using a Volterra series representation; this series is a generalization of the power series. In a now classic report, Wiener applied this analysis technique[12] to find the response of a nonlinear device to noise.[13] Bose has carried the theory further.[14] Following a series of lectures by Wiener,[15] the theoretical framework, higher-dimensional transforms, and optimization with Gaussian inputs were considered by Brilliant,[16] George,[17] and Chesler,[18] respectively. Barrett[19] has treated statistical inputs. The synthesis problem has been examined by Van Trees,[20] who also applied the method to phase-locked loops.[21] The technique has been extended to discrete systems,[22,23,24] and a class of time-variant systems.[24,25] More recently the theory of the convergence of the series has been treated.[26] This work relies more on George's work on the higher-dimensional transform theory.[17]

Even though much work has been done in this area, the Volterra series has not found a wide application in solving nonlinear system problems due to several reasons; if the rate of convergence is not rapid, the higher-degree terms, which are cumbersome to handle, cannot be neglected; hence, it cannot conveniently represent gross nonlinearities. It is not simple to invert the multidimensional transforms to the time domain, and it is not a useful technique to determine the stability of a nonlinear differential equation.

The Volterra series method does, however, offer certain distinct advantages in analyzing transistor distortion. Since transistor distortion is frequency dependent, the power series is inadequate to characterize it; the Volterra series does indeed represent frequency dependent systems. The nonlinearities in the transistors under consideration are extremely small so that the second- and third-degree terms suffice to

characterize them. Since the output corresponding to sinusoidal input signals is of interest, there is no need to find the inverse of the higher-dimensional transforms; the output can be expressed in terms of the transform of the kernel. The higher-dimensional transforms of the kernel are complex numbers when $s_i = j\omega_i$, where s_i is the complex variable in the transform domain; hence, these kernels can be numerically evaluated using the computer (see Section IV). Moreover, for a slightly simpler model closed form ac expressions can be derived. Since the kernels retain phase information, this approach will be useful for the AM-to-PM conversion problem at IF frequencies. Finally, in an amplifier two or more transistors are cascaded; the nonlinear behavior of such cascaded transistors is a significant problem. The Volterra series approach can be easily extended to study such cascaded transistors.

II. AN INTRODUCTION TO VOLTERRA SERIES REPRESENTATION

A brief exposition of Volterra series with pertinent reference to the problem under consideration is presented below. For further details the reader is referred to the references cited.

Consider a simple memoryless nonlinear system described by the following power series; let $y(t)$ be the output and $x(t)$ the input; the system is represented by

$$y(t) = c_1x(t) + c_2[x(t)]^2 + c_3[x(t)]^3, \tag{1}$$

where c_1, c_2, c_3 are constants. For a time-invariant system with memory (capacitors and inductors in an electrical network), the linear term $\{c_1x(t)\}$ is replaced by the convolution integral $(x(t) = 0; t < 0)$

$$y_1(t) = \int_0^t c_1(t - \tau)x(\tau)\, d\tau. \tag{2}$$

In the transform domain, (2) may be written

$$Y_1(s) = C_1(s)X(s). \tag{3}$$

This transform domain representation of the system $[C_1(s)]$ has been an invaluable aid to the communication engineers since it brings into focus the frequency behavior of the system.

A generalization of the second-degree term, $c_2[x(t)]^2$, is the double convolution integral

$$y_2(t) = \int_0^t \int_0^t c_2(t - \tau_1, t - \tau_2) \prod_{i=1}^{2} x(\tau_i)\, d\tau_i . \tag{4}$$

The output depends on the past values of the input; the above expression involves a product of the input with itself, thus representing a quadratic system. $c_2(t - \tau_i , t - \tau_2)$ is known as the second-degree Volterra kernel.

A two-dimensional Laplace transform can be defined for (4) after introducing dummy variables t_1 and t_2. As shown in Appendix A, (4) becomes

$$Y_2(s_1 , s_2) = C_2(s_1 , s_2) \prod_{i=1}^{2} X(s_i). \tag{5}$$

When two sinusoidal signals at frequencies f_a and f_b are applied (Appendix A), the output at the harmonic frequency $f_a \pm f_b$ is given by $[| C_2(f_a \pm f_b) | \cos (2\pi(f_a \pm f_b)t + \phi_{a\pm b})]$. Since in general $C_2(f_a , f_b)$ will not be equal to $C_2(f_a , -f_b)$, different values of distortion at different harmonic frequencies are directly reflected in the kernel. Moreover, as in the power series case, the $2f$ product is less by a factor of two.

Likewise, the third-degree term $[c_3(x(\tau))^3]$ can be generalized to a triple convolution integral;

$$y_3(t) = \int_0^t \int_0^t \int_0^t C_3(t - \tau_1 , t - \tau_2 , t - \tau_3) \prod_{i=1}^{3} x(\tau_i)\, d\tau_i . \tag{6}$$

In the transform domain (6) may be written

$$Y_3(s_1 , s_2 , s_3) = C_3(s_1 , s_2 , s_3) \prod_{i=1}^{3} X(s_i). \tag{7}$$

The magnitude of the signal at the harmonic frequency $f_a + f_b - f_c$ due to the three fundamental signals at f_a, f_b and f_c is given by $| C_3(f_a , f_b , -f_c) |$. The constants like 1/4 for a '$3f_a$' product are the same as obtained from the power series approach.

Later in the paper (in Section IV) the cascade relations in the transform domain are frequently used; their physical significance is discussed in detail in Section VI. (See also Fig. 1.) The cascade formulae and the procedure for deriving them are given in Appendix A.

The second and third harmonic distortion are defined as the second and third harmonic power in dBm, respectively, when the fundamental power at the output of the transistor is at zero dBm (one milliwatt). In the analysis of the model in Section IV, the output voltage is expressed in terms of a Volterra series of the input voltage. Thus, the kernels $C_1(s_1)$, $C_2(s_1 , s_2)$, and $C_3(s_1 , s_2 , s_3)$ are the voltage transfer ratios; for a given load R_L, the second and the third harmonic distortion in dBm are given by the following expressions:

$$M_{2_{a\pm b}} = 20 \log \frac{1}{2} \frac{|\, C_2(f_a \pm f_b) \,| \sqrt{10^{-3} R_L}}{|\, C_1(f_a) \,|\, |\, C_1(\pm f_b) \,|} \tag{8}*$$

$$M_{3_{a\pm b\pm c}} = 20 \log \frac{1}{4} \frac{|\, C_3(f_a \pm f_b \pm f_c) \,| \, 10^{-3} R_L}{|\, C_1(f_a) \,|\, |\, C_1(\pm f_b) \,|\, |\, C_1(\pm f_c) \,|}. \tag{9}*$$

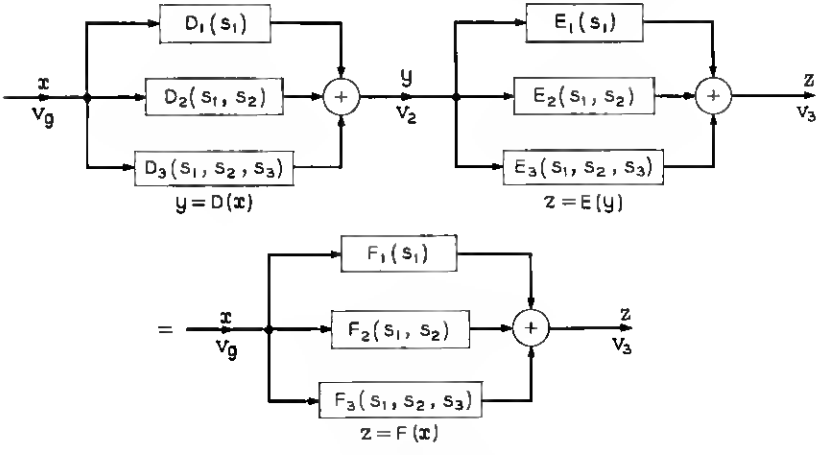

Fig. 1 — Two cascaded systems.

III. THE JUNCTION TRANSISTOR NONLINEAR MODEL

A model is a simple but realistic representation of a physical phenomenon in terms of measurable parameters such that the phenomenon can be analyzed, and controlled if possible. The linear equivalent circuit of a transistor is one such example. In reality, several elements of the transistor equivalent circuit are not linear but are linearized versions of nonlinear functions; they are the first-degree terms of the Taylor's series expansion of the nonlinear functions. Hence, a logical way to develop the nonlinear model is to consider the second- and third-degree terms of the Taylor's series expansion; thus, the emitter resistance (exponential nonlinearity), current gain (h_{FE} and avalanche nonlinearity), and the collector capacitance (collector capacitance nonlinearity) have been represented by nonlinear voltage dependent current generators whose parameters are higher-degree Taylor's series terms. This approach has another advantage in that it is difficult to measure the nonlinearities since they are small; but, it is not too difficult to measure the overall functions and to curve fit with the known theoretical

* The factors $\frac{1}{2}$ and $\frac{1}{4}$ normalize the distortion to $2f$ and $3f$ products.

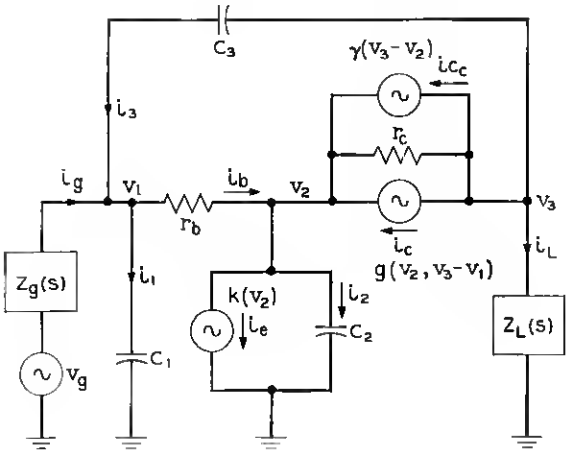

Fig. 2 — Common-emitter nonlinear equivalent circuit.

or empirical relations. These nonlinearities are superimposed on the linear equivalent circuit (Fig. 2). The nonlinearities are described next.

3.1 *Exponential Nonlinearity*

The emitter current, I_E, is related to the emitter voltage, V_2, by the exponential relation

$$I_E = A\left[\exp\left(q\frac{V_2}{KT}\right) - 1\right] + B, \tag{10}$$

where K = Boltzmann's constant,

q = electron charge in coulombs,

T = Temperature in degrees Kelvin,

and A and B are constants which depend on the transistor parameters (Ref. 27; p. 181, p. 249). An experimental curve of the emitter current I_E and the emitter-to-base voltage V_{be} is shown in Fig. 3. This nonlinearity is expressed as a voltage-dependent current generator by a Taylor's series expansion of (10) as follows:

$$i_e = K(v_2) = K_1 v_2 + K_2 v_2^2 + K_3 v_2^3, \tag{11}$$

where the Taylor's series coefficients are derived in terms of known parameters, the emitter resistance r_e, and the emitter bias current I_E; i.e.,

$$K_1 = \frac{1}{r_{e_1}} ; \quad K_2 = \frac{1}{2(r_{e_1})^2} \frac{1}{I_E} ; \quad K_3 = \frac{1}{6} \frac{1}{(I_E)^2} \frac{1}{(r_{e_1})^3}. \tag{12}$$

3.2 *Avalanche and h_{FE} Nonlinearity*

The collector current is a nonlinear function of the emitter current at higher values of current (h_{FE} nonlinearity) and of the collector-to-base voltage at higher values of voltage (avalanche nonlinearity).[27] h_{FE}, the ratio of I_C to I_B, is plotted as a function of collector current I_C in Fig. 4. It is seen that the following empirical relation[6] matches the experimental result (Fig. 4):

$$h_{FE} = \frac{h_{FE\,\max}}{1 + a \log^2 \dfrac{I_C}{I_{C\,\max}}}, \tag{13}$$

where $h_{FE\,\max}$ is the maximum value of h_{FE}, $I_{C\,\max}$ is the value of I_C at which $h_{FE\,\max}$ occurs, and a is a constant.

The avalanche nonlinearity is due to avalanche multiplication which occurs at higher collector-to-base voltage. It is determined from the collector characteristic which is a plot of collector current (I_C) and collector-to-emitter voltage (V_{CE}), (Fig. 5). The empirical Miller's avalanche multiplication factor is given by

$$\frac{1}{1 - \left(\dfrac{V_{CE}}{V_{CEO}}\right)^n}, \tag{14}$$

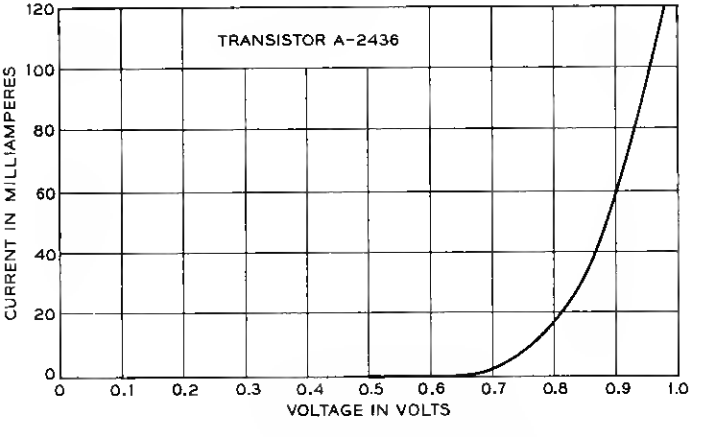

Fig. 3 — Exponential nonlinearity — measured curve.

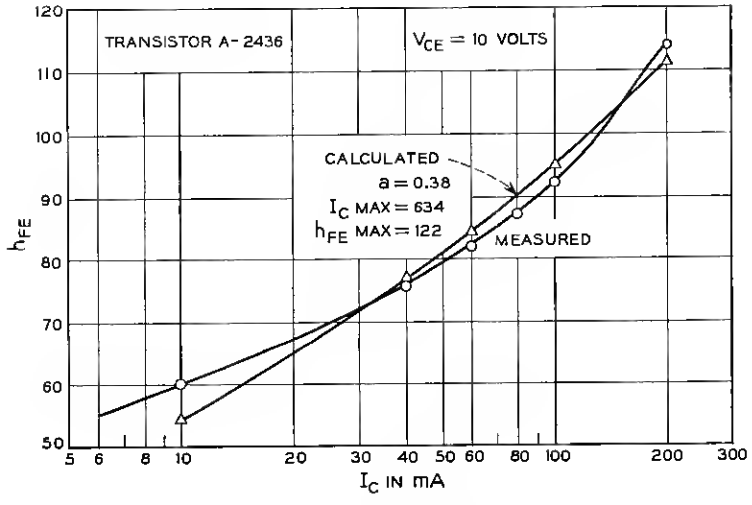

Fig. 4—h_{FE} nonlinearity — calculated and measured curves.

where V_{CEO} is the sustained voltage, and the exponent n is determined by experiment. From expressions (13) and (14), the ratio $I_C v_S I_E$ is given by

$$\frac{I_C}{I_E} = \frac{h_{FE\,\max}}{1 + h_{FE\,\max} + a \log^2 \left(\frac{I_C}{I_{C\,\max}}\right)} \cdot \frac{1}{1 - \left(\frac{V_{CB}}{V_{CBO}}\right)^n}, \tag{15}$$

where $V_{CBO} = V_{CEO}/n\sqrt{1-\alpha}$ and $V_{CB} \cong V_{CE}$.

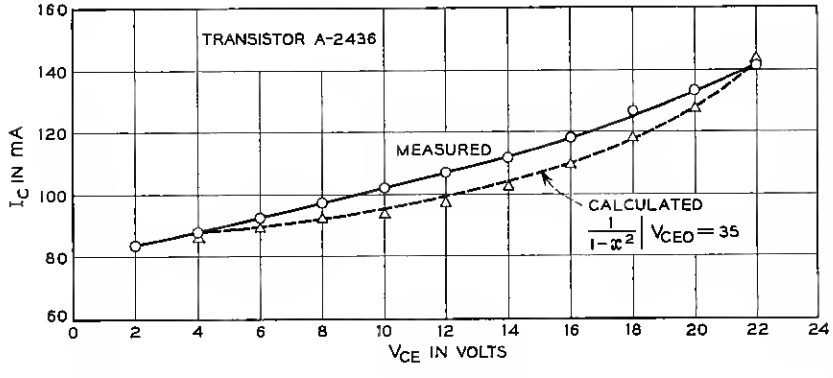

Fig. 5—Avalanche nonlinearity — calculated and measured curves.

The ac i_e can be expressed in terms of i_e and $v_{cb}[v_3 - v_1]$ by a Taylor's series expansion of (15). Since i_e is a function of emitter voltage v_2, i_e is represented by a current generator $g(v_2, v_3 - v_1)$; for convenience in notation it is separated into a linear term $g_1(v_2, v_3 - v_1)$, a second-degree term $g_2(v_2, v_3 - v_1)$ and a third-degree term $g_3(v_2, v_3 - v_1)$. The linear term equals $\hat{M}_0(\alpha_1 K_1)v_2 + \hat{M}_1(v_3 - v_1)$. The second-degree term is given by $\alpha_2\hat{M}_0K_1^2(v_2)^2 + m_2(v_3 - v_1)^2 + (\alpha_1\hat{M}_1)K_1v_2(v_3 - v_1)$. The coefficients α_1, α_2, $\hat{M}_1$, m_2, etc., and the third-degree term are given in Appendix B.

3.3 *Collector Capacitance Nonlinearity*

The collector capacitance is a nonlinear function of collector-to-base voltage (V_{CB}) since the depletion layer width is a function of V_{CB}. The exact functional relationship is determined by plotting the common-base imaginary part of h_{22} as a function of collector-to-base voltage (V_{CB}) as shown in Fig. 6.[9] It is evident from the figure that C_c follows the 1/3 voltage law (Ref. 19; Equation 5-96);

$$C_c = k(V_{CB})^{-1/3}. \tag{16}$$

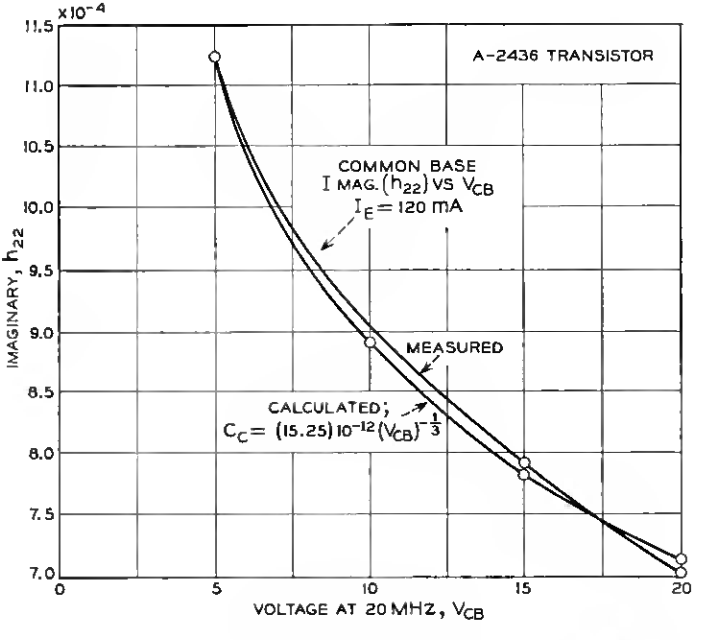

Fig. 6 — Collector capacitance nonlinearity — calculated and measured curves.

This nonlinearity is represented as a frequency (differentiation) and voltage-dependent current generator as follows:

$$i_{c_c} = \gamma(v_3 - v_1)$$

$$= \gamma_1 \frac{d}{dt}(v_3 - v_1) + \gamma_2 \frac{d}{dt}(v_3 - v_1)^2 + \gamma_3 \frac{d}{dt}(v_3 - v_1)^3, \quad (17)$$

where $\gamma_1 = C_c$, and where γ_2 and γ_3 are known from (16).

The above nonlinear current generators are incorporated in the linear equivalent circuit as shown in Fig. 2. The linear equivalent circuit parameters are obtained from the equivalent circuit characterization. They can, for example, he computed from the h-parameters at different frequencies. In general, the distortion is not a critical function of the linear parameters. (Figs. 14 to 17).

All the nonlinear coefficients (K_2, α_2, m_2, etc.) are easily obtained from a simple computer program. The parameters to he specified along with typical values for transistor type A-2436 are listed in Appendix C.

IV. THE VOLTERRA KERNELS FOR THE NONLINEAR MODEL

The Volterra series method is applied to the model to compute the second and the third harmonic distortion. The voltage at each node is a nonlinear frequency-dependent function of the input voltage. Each nodal voltage is expressed hy a Volterra series expansion of the generator voltage; since the nonlinearities are small only three terms are considered. The kernels at each node are determined from Kirchoff's current equations.

4.1 *Nodal Equations*

The Kirchoff's current law is applied at each node; the currents are next expressed in terms of the generator voltage v_g, the three nodal voltages v_1, v_2, and v_3, and the known linear and nonlinear parameters. The impedances are represented by their transforms and o denotes that it operates on the voltage across it. The nodal equations are given helow.

$$\frac{1}{Z_g(s)} o\,(v_g - v_1) + (sC_3)\, o\,(v_3 - v_1) = (sC_1)\, o\, v_1 + \frac{1}{r_b} o\,(v_1 - v_2), \quad (18)$$

$$\frac{1}{r_b} o\,(v_1 - v_2) = K(v_2) + (sC_2)\, o\, v_2 + \left(\frac{1}{r_c}\right) o\,(v_2 - v_3) - \gamma(v_3 - v_2) - g(v_2, v_3 - v_1), \quad (19)$$

$$-\gamma(v_3 - v_2) + \frac{1}{r_e}(v_2 - v_3) - g(v_2, v_3 - v_1) = (sC_3) \; o \; (v_3 - v_1) + \left(\frac{1}{Z_L(s)}\right) o \; v_3 , \tag{20}$$

where $K(v_2)$, $\gamma(v_2 - v_3)$ and $g(v_2, v_3 - v_1)$ are the nonlinear current generators.

4.2 *Solution Using Volterra Series*

Since each nodal voltage is to be expressed in terms of three Volterra kernels, there are nine unknown Volterra kernels to be determined from the three equations. The problem of solving for nine unknowns from three equations is resolved by noting that the polynomials x, x^2 and x^3 are linearly independent; hence, each degree term is separately and successively solved. The linear kernels are first determined; then the second-degree kernels are determined in terms of the linear kernels; lastly, the third-degree kernels are evaluated in terms of the first- and second-degree kernels.

Let $A_1(s)$, $B_1(s)$, $C_1(s)$ denote the transforms of the linear kernels at nodes one, two and three, respectively. From the nodal equations (18) to (20), the following vector matrix equation is derived.

$$\begin{Bmatrix} \frac{1}{Z_g(s)} \\ 0 \\ 0 \end{Bmatrix} = P_E(s) \begin{Bmatrix} A_1(s) \\ B_1(s) \\ C_1(s) \end{Bmatrix}, \tag{21}$$

where

$$P_E(s) = \begin{bmatrix} \frac{1}{Z_g(s)} + s(C_3 + C_1) + \frac{1}{r_b} & -\frac{1}{r_b} & -sC_3 \\ -\frac{1}{r_b} + m_1 & \frac{1}{r_b} + sC_2 + \frac{1}{r_c} + K_1(1-\alpha) + s\gamma_1 & -\frac{1}{r_c} - m_1 - s\gamma_1 \\ -sC_3 - m_1 & -\frac{1}{r_c} + \alpha_1 K_1 - s\gamma_1 & \frac{1}{r_c} + sC_3 + \frac{1}{Z_L(s)} + m_1 + s\gamma_1 \end{bmatrix}. \tag{22}$$

Equation (21) is solved by inverting matrix $P_E(s)$ and post-multiplying by the vector

$$\begin{Bmatrix} \frac{1}{Z_g(s)} \\ 0 \\ 0 \end{Bmatrix}.$$

For a given frequency $s = j\omega$, the computation is done numerically.

The second-degree terms are equated next in (18) to (20). There are two types of second-degree terms; those arising from the unknown second-degree kernels [for example, $(s_1 + s_2)C_1A_2(s_1, s_2)$] and those arising from the known nonlinear coefficients and the known linear kernels [for example, $K_2 \prod_{i=1}^{2} B_1(s_i)$]. The terms associated with the unknown second-degree kernels are the same as were associated with the unknown linear kernels in (21), but at the harmonic frequency $(s_1 + s_2)$. The following vector matrix equation is obtained for the second-degree kernels:

$$\begin{Bmatrix} 0 \\ [\hat{g}_2(B_1, C_1 - A_1) \\ +\gamma_2(C_1 - B_1) - K_2(B_1)] \\ [-\hat{g}_2(B_1, C_1 - A_1) \\ -\hat{\gamma}_2(C_1 - B_1)] \end{Bmatrix} = P_E(s_1 + s_2) \begin{Bmatrix} A_2(s_1, s_2) \\ B_2(s_1, s_2) \\ \\ C_2(s_1, s_2) \\ \\ \end{Bmatrix}, \tag{23}$$

where $\hat{g}_2$ and $\hat{\gamma}_2$ represent the second harmonic contribution due to $g_2(v_2, v_3 - v_1)$ and $\gamma_2(v_3 - v_2)$; hence,

$$\begin{aligned} \hat{g}_2(B_1, C_1 - A_1) = [\alpha_1 K_2 + \alpha_2 K_1^2] \prod_{i=1}^{2} B_1(s_i) \\ + \frac{\alpha_1 M_1 K_1}{2} [B_1(s_1)[C_1(s_2) - A_1(s_2)] \\ + B_1(s_2)[C_1(s_1) - A_1(s_1)]] \\ + m_2 \prod_{i=1}^{2} [C_1(s_i) - A_1(s_i)] \end{aligned} \tag{24}$$

$$\hat{K}_2(B_1) = K_2 \prod_{i=1}^{2} B_1(s_i) \tag{25}$$

$$\hat{\gamma}_2(C_1 - B_1) = K_2(s_1 + s_2)\gamma_2 \prod_{i=1}^{2} [C_1(s_i) - B_1(s_i)]. \tag{26}$$

$P_E(s_1 + s_2)$ is the matrix $P_E(s)$ with s replaced by $(s_1 + s_2)$.

The vector on the left side of (23) is known. Thus, the unknown kernels are determined by inverting the matrix $P_E(s_1 + s_2)$ and post-multiplying by the vector on the left-hand side of (23). When $s_1 = j\omega_5$, the inversion of the matrix and the post multiplication by the vector can be done numerically.

The procedure for obtaining the third-degree kernels is almost the same; the significant difference is that the vector on the left side not only contains terms arising from the third-degree nonlinear parameters but also includes second-degree coefficients which give rise to third-degree terms by the interaction of the first- and the second-degree kernels. These interaction terms are denoted by $\hat{K}_{23}$, $\hat{g}_{23}$, $\hat{\gamma}_{23}$, respectively. For example, $K_3(B_1) = K_3 \prod_{i=1}^{3} B_1(s_i)$, whereas $K_{23} = 2k_2 B_1(s_1) B_2(s_2 , s_3)$ which shows the interaction of tbe first- and tbe second-degree kernels. The third-degree kernels are derived from the following equations:

$$\begin{Bmatrix} 0 \\ [\hat{g}_3(B_1 , C_1 - A_1) + \hat{\gamma}_3(C_1 - B_1) \\ \quad - \hat{K}_3(B_1) + \hat{g}_{23} + \hat{\gamma}_{23} + \hat{K}_{23}] \\ [-\hat{g}_3(B_1 , C_1 - A_1) - \hat{\gamma}_3(C_1 - B_1) \\ \quad - \hat{g}_{23} - \hat{\gamma}_{23}] \end{Bmatrix}$$

$$= P_E(s_1 + s_2 + s_3) \begin{Bmatrix} A_3(s_1 , s_2 , s_3) \\ B_3(s_1 , s_2 , s_3) \\ C_3(s_1 , s_2 , s_3) \end{Bmatrix} , \qquad (27)$$

where $\hat{g}_3$, $\hat{g}_{23}$ are given in Appendix B.

A computer program has been developed which calculates the kernels and the second and the third harmonic distortion. It uses existing programs to invert the matrix $P_E(s)$. The nonlinear coefficients are computed from the known and measured parameters. Computed and measured results at different currents are given in Fig. 7. The program has been extended to common-base and common-collector configurations.

V. SIMPLIFIED DISTORTION EXPRESSIONS, THEIR PHYSICAL SIGNIFICANCE AND COMPARISON WITH EXPERIMENTAL RESULTS

Another advantage of the Volterra series method is that it permits derivation of closed-form expressions for second and third harmonic distortion. These equations show the interaction between the various nonlinear parameters and the effect of frequency.

The model includes the base resistance (r_b), the emitter resistance (r_e), the diffusion capacitance (C_2), the load (R_L) and the source impedances $Zg(s)$, and three nonlinearities, namely, exponential, avalanche, and h_{FE} nonlinearities. In the computer program C_{be} , C_{b} ,

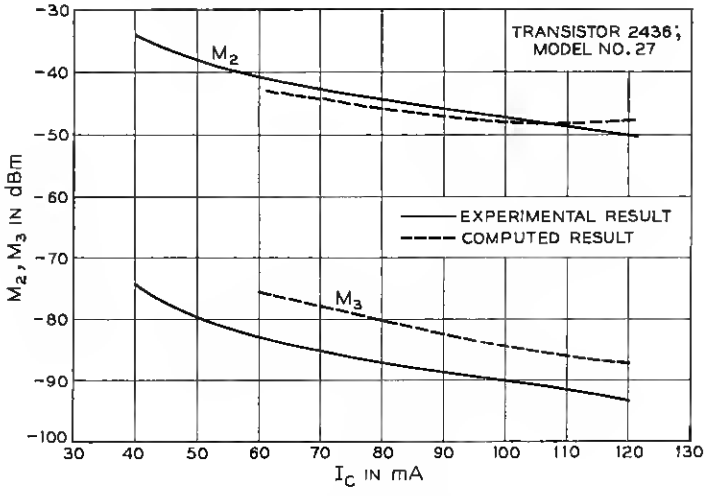

Fig. 7—Comparison of experimental and computed results.

r_e , C_c , m_1 and collector capacitance nonlinearity have been taken into account. The expressions given below are for the common-emitter configuration.

5.1 *The Second Harmonic Distortion Term*

The second harmonic distortion in dBm (8) is given by

$$M_{2a\pm b} \approx 20 \log \frac{1}{2}\sqrt{\frac{10^{-3}}{R_L}}\left|\left[\frac{(r_b + Z_e(\underline{s}))\cdot(K_1 + \underline{s}C_2) + 1}{(r_b + Z_e(\underline{s}))\cdot[K_1(1-\alpha_1) + \underline{s}C_2] + 1}\right]\right.$$
$$\cdot\left[\frac{\alpha_2}{(\alpha_1)^2} - \hat{M}_1\left(R_L + \frac{\underline{s}C_2}{2}\frac{r_b}{\alpha_1 K_1}\right) + m_2\prod_{i=1}^{2}\left(R_L + \frac{s_i C_c r_b}{\alpha_1 K_1}\right)\right.$$
$$\left.\left. + \frac{K_2}{\alpha_1 K_1^2}\left(\frac{(Z_e(\underline{s}) + r_b)\cdot\underline{s}C_2 + 1}{(Z_e(\underline{s}) + r_b)\cdot(K_1 + \underline{s}C_2) + 1}\right)\right]\right| \tag{28}$$

where $s_1 = j\omega_a$, $s_2 = \pm j\omega_b$ and $\underline{s} = j\omega_a \pm j\omega_b$.

5.2 *The Third Harmonic Distortion Term*

In the third harmonic distortion term given below, the interaction terms due to the first- and the second-degree kernels have not heen included mainly to reduce the complexity; in certain cases, they may be significant.

$$M_{3a\pm b\pm c} \approx 20 \log \frac{1}{4}\frac{10^{-3}}{R_L}\left|\left[\frac{(r_b + Z_e(\underline{s}))\cdot(\underline{s}C_2 + K_1) + 1}{(r_b + Z_e(\underline{s}))\cdot(K_1(1-\alpha_1) + \underline{s}C_2) + 1}\right]\right.$$

$$\cdot\left[\frac{\alpha_3}{(\alpha_1)^3}+\hat{M}_1\left(R_L^2+\frac{2}{3}\frac{R_L\underline{s}C_2r_b}{\alpha_1K_1}+\frac{1}{3}\frac{\overline{s_is_j}C_2^2r_b^2}{(\alpha_1K_1)^2}\right)-m_3\prod_{i=1}^{3}\left(R_L+\frac{s_iC_2r_b}{\alpha_1K_1}\right)\right.$$

$$+\frac{K_3}{(\alpha_1K_1)^3}\frac{\alpha_1[(r_b+Z_e(\underline{s}))(\underline{s}C_2)+1]}{(r_b+Z_e(\underline{s}))\cdot(\underline{s}C_2+K_1)+1}+\frac{2\alpha_2K_2}{(\alpha_1)^3K_1^2}$$

$$\left.-\frac{\alpha_2\hat{M}_1}{(\alpha_1)^3}\left[\alpha_1R_L+\frac{\underline{s}}{3}\frac{C_2r_b}{(K_1)^3}\right]\right]\Bigg|, \tag{29}$$

where $s_1 = j\omega_a$, $s_2 = j\omega_b$, $s_3 = \pm j\omega_c$ and $\underline{s} = s_1 + s_2 + s_3$ and $\overline{s_is_j} = s_1s_2 + s_2s_3 + s_3s_1$.

5.3 *Physical Interpretation of the Distortion Terms*

The interaction of different nonlinearities and their dependence on load impedance, source impedance, bias currents, bias voltage and frequency is indeed somewhat complex. However, the closed form expressions derived above give a general qualitative picture which will be discussed now.

5.3.1 *Effect of Frequency*

It is important to know the effect of frequency on distortion. Tbe distortion depends not only on the frequencies of the fundamental tones but also on the harmonic frequency of interest. As sbown in Fig. 8,

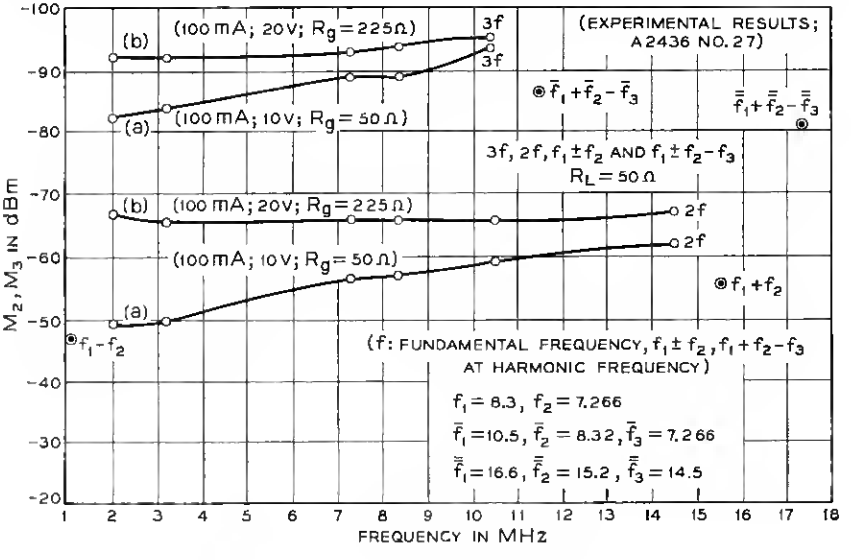

Fig. 8—Variation of M_2, M_3 with frequency.

M_2 due to $a + b$ product is better than M_2 of $a - b$ product by 10 dB with the two tones at 8.32 and 7.266 MHz. These measurements were made with the transistor biased at 100 mA, 10V and with $R_L = 50\Omega$ and $R_g = 50\Omega$. In curve (a) of Fig. 8, the fundamental tone was increased from 2 MHz to 10.5 MHz and signals at $2f$ and $3f$ were measured. It is seen that both M_2 and M_3 improved with increase in frequency. A theoretical explanation on the basis of dominant terms (in this range of parameter values) in (28) and (29) is given below. In (28) as well as in (29) the terms in brackets are multiplied by a frequency-dependent term

$$\frac{(r_b + R_g)(K_1 + \underline{s}C_2) + 1}{(r_b + R_g)(K_1(1 - \alpha_1) + \underline{s}C_2) + 1}.$$

In this range of frequency ($\underline{s}$ = harmonic frequency), if $K_1(1 - \alpha_1) \leqq | \underline{s}C_2 |$ and if $| (r_b + R_g)\underline{s}C_2 | > 1$ but $K_1 > | (\underline{s}C_2) |$, then the above term reduces to $K_1/\underline{s}C_2$ which decreases with increase in frequency. However, the avalanche terms ($\hat{M}_2$, $\hat{M}_3$, etc.) involve the terms $\underline{s}C_2$ [in (28) and (29)] and S_iC_2 in the numerator. Thus, if the avalanche terms are dominant, as at higher voltages, there should be no net contribution due to avalanche terms alone. The exponential terms [$K_2/(K_1)^2$ and $K_3/(K_1)^3$] are multiplied by the factor

$$\frac{(r_b + R_g)\cdot \underline{s}C_2 + 1}{(r_b + R_g)\cdot(K_1(1 - \alpha_1) + \underline{s}C_2) + 1}.$$

This term is independent of frequency if $(\underline{s}C_2(r_b + R_g) + 1) > 1$. Thus the above discussion shows that distortion will improve with increase in frequency at lower voltages and if $| \underline{s}C_2(r_b + R_g) + 1 | < 1$. To verify this statement, the voltage was increased to 20 volts and the input resistance changed to 225Ω. The plots of M_2 and M_3 with frequency, as measured, are given in curves labeled (b) in Fig. 8. It is seen that M_2 and M_3 do not improve with increase in frequency. The small improvement can be attributed to the h_{FE} terms.

In general, increase in frequency increases distortion; this is especially true for the common base configuration. But as shown above, for certain ranges of frequency and certain values of source impedance, distortion can improve with frequency.

5.3.2 *Effect of Load Resistance, R_L*

The load resistance is an external parameter which the circuit designer can vary; hence, it is useful to know its effect on distortion. The second and the third harmonic terms are multiplied by $1/\sqrt{R_L}$ and $1/R_L$

terms, respectively; it shows that the distortion can be reduced by increasing R_L. However, the avalanche terms $\hat{M}_1$, $\hat{M}_2$, and $\hat{M}_3$ are multiplied by the R_L term, so that increasing R_L will increase the contribution from the avalanche terms. Thus, an increase in R_L may increase distortion or reduce it due to cancellation. (The contribution from the collector capacitance terms also increases with increase in load (R_L).) Because of the above interaction, for a given set of parameters and input frequencies and the harmonic frequency of interest there exists an optimum load R_L; this, of course, can be determined using the computer program. In Fig. 9, the measured values of M_2 and M_3 at different values of R_L are plotted; in both cases increasing R_L reduces distortion until the optimum value is reached and then distortion increases with increase in R_L.

5.3.3 *Effect of Source Impedance, $Z_g(s)$*

Source impedance is another important external parameter. The source impedance affects the exponential nonlinearities K_2/K_1^2 in (28) and K_3/K_1^3 in (29) by the factor

$$\frac{(r_b + Z_g(s))sC_2 + 1}{(r_b + Z_g(s)) \cdot [sC_2 + K_1(1 - \alpha_1)] + 1}.$$

At low frequencies, this nonlinearity is reduced by the factor $1/[(1 - \alpha)(R_g + r_b)K_1 + 1]$. Thus, an increase in R_g will reduce distortion from this source. However, the contribution from other nonlinearities are increased by

$$\frac{1 + K_1(R_g + r_b)}{1 + K_1(R_g + r_b)(1 - \alpha_1)}.$$

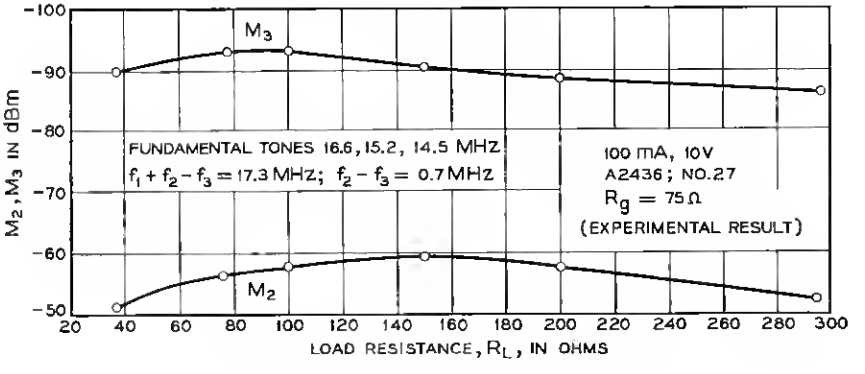

Fig. 9—Variation of M_2, M_3 with load resistance.

It is seen from this expression that if $K_1(R_g + r_b)(1 - \alpha_1)$ is greater than 1, the other nonlinearities are not affected by the increase in R_g. Thus, if the exponential term is dominant, increasing R_g reduces distortion at low frequencies. At higher harmonic frequencies if $| \underline{s}C_2(Z_g(\underline{s}) + r_b) | > 1$, the distortion terms are independent of the source impedance since the $[r_b + Z_g(\underline{s})]$ term in the numerator and denominator cancel. This is well illustrated in the measured results of Fig. 10. The second harmonic frequency heing 0.7 MHz, $| \underline{s}C_2(R_g + r_b) |$ is not much greater than one up to $R_g = 100\Omega$; hence, the second harmonic distortion improves with increase in source resistance up to 140Ω. Further increase in R_g does not cause much change in distortion. The third harmonic frequency is 17.3 MHz; hence, a change in R_g does not affect M_3 appreciahly. $(| (\underline{s}C_2) \cdot (R_g + r_b) | > 1)$

5.3.4 *Effect of Bias Current*

Increase in hias current usually reduces distortion due to the following reasons. The increase in emitter hias current reduces the exponential terms

$$\frac{K_2}{(K_1)^2}\left(\alpha \frac{1}{I_E}\right) \quad \text{and} \quad \frac{K_3}{(K_1)^3}\left[\alpha \frac{1}{(I_E)^2}\right].$$

Fig. 11 shows the effect of bias current on h_{FE} terms; α_2 decreases with increase in I_C by

$$\frac{1}{I_C} \log \left(\frac{I_C e}{I_{C\,\max}}\right);$$

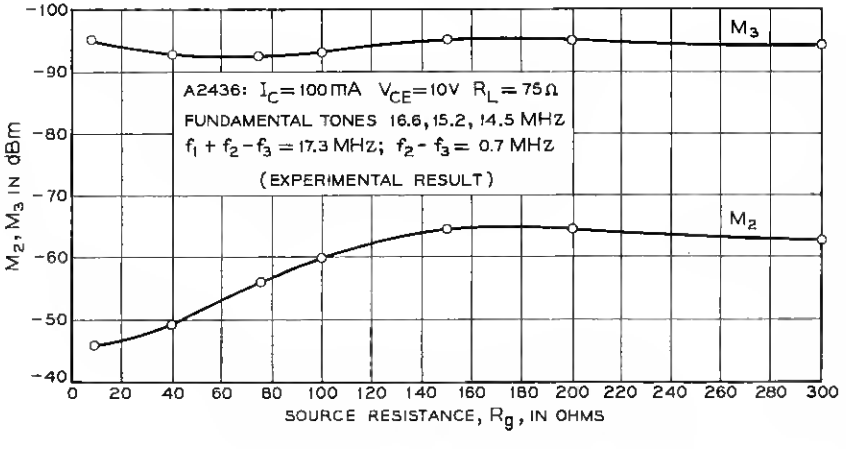

Fig. 10—Variation of M_2, M_3 with source resistance.

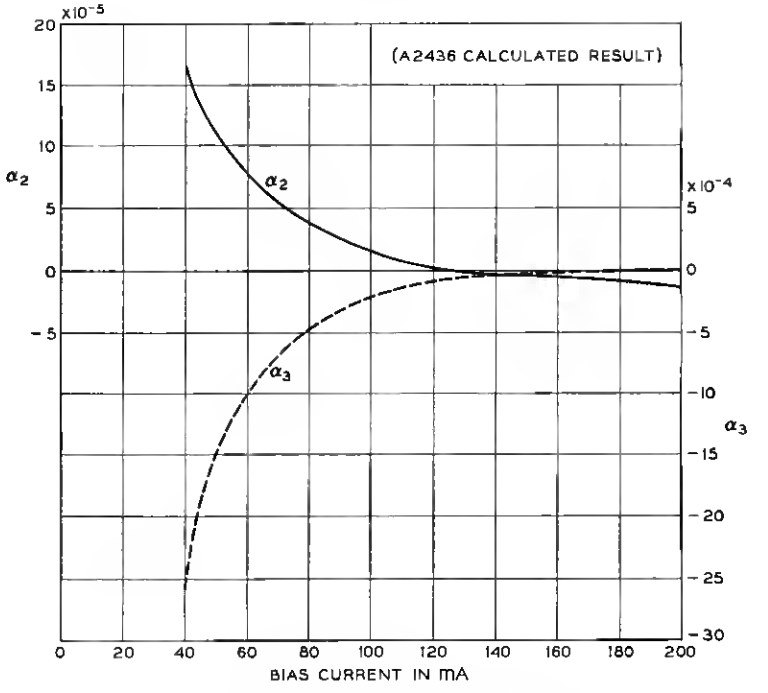

Fig. 11 — Variation of α_2 , α_3 with bias current.

it becomes zero at $I_C = I_{C\,max}/e$, and then becomes negative, and increases with further increase in I_C . The coefficient α_3 decreases with bias current I_E . Thus, in general, an increase in bias current has the effect of reducing both the second and third harmonic distortion (Fig. 7) (at least until $\alpha_2 = 0$).

5.3.5 *Effect of Bias Voltage*

Whereas exponential and h_{FE} terms are functions of bias current, the avalanche and collector capacitance nonlinearities are affected by the bias voltage. The coefficient $\hat{M}_2$ increases with the voltage; but $\hat{M}_1$ and $\hat{M}_3$ increase much more rapidly (Fig. 12). (Both the collector capacitance nonlinear coefficients γ_2 , γ_3 decrease with tbe increase in bias voltage.) The effects of change in bias voltage are especially pronounced at higher load resistance since avalanche (and collector capacitance) terms become dominant. The third harmonic distortion decreases more with the increase in voltage (Fig. 13) than the second harmonic distortion does.

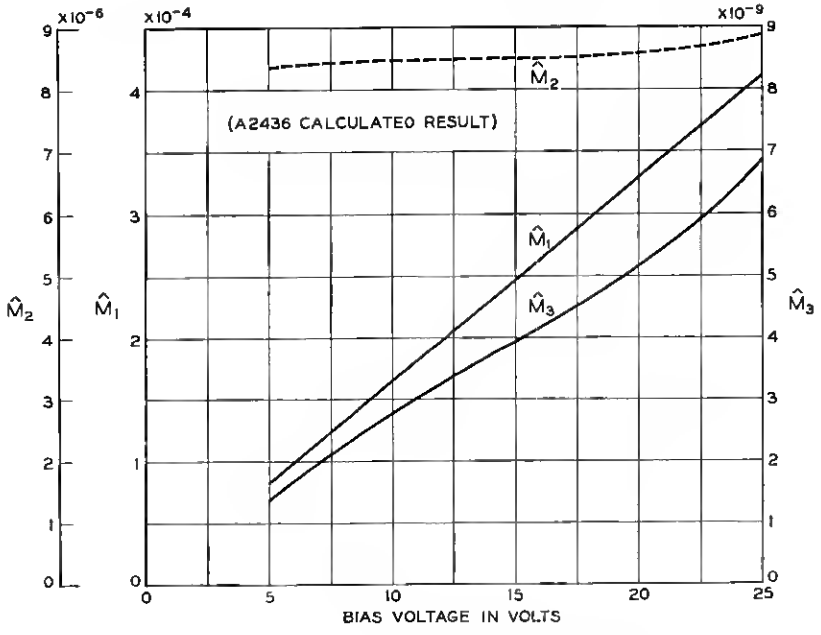

Fig. 12 — Variation of $\hat{M}_1$, $\hat{M}_2$, $\hat{M}_3$ with bias voltage.

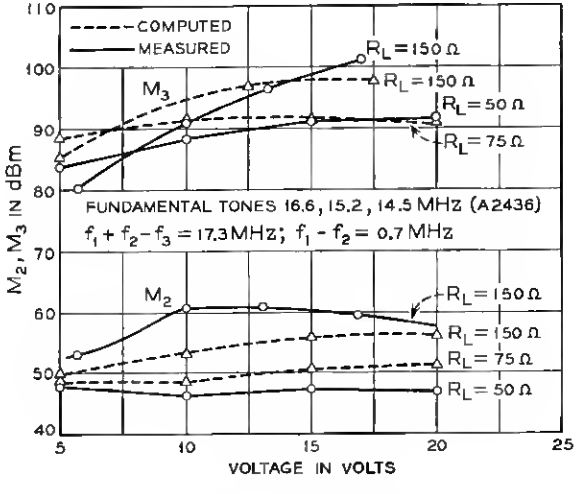

Fig. 13 — Variation of M_2, M_3 with voltage at 100 mA.

The physical significance of the closed form expressions has been qualitatively discussed. Precise quantitative estimates can and have been obtained using the computer program. For example, the effect of varying linear parameters by fifty percent of their original values was studied. The results show that the distortion does not critically depend on the linear parameters (Figs. 14 to 17). The other transistor parameters such as $I_{C\,max}$, V_{CEO}, n, etc., can also he varied.

VI. ANALYSIS OF CASCADED TRANSISTORS

It is often stated that in a multi-stage amplifier, the output stage alone determines the over-all distortion. Even though this statement is true to some extent, it is frequently found in practice that the effects

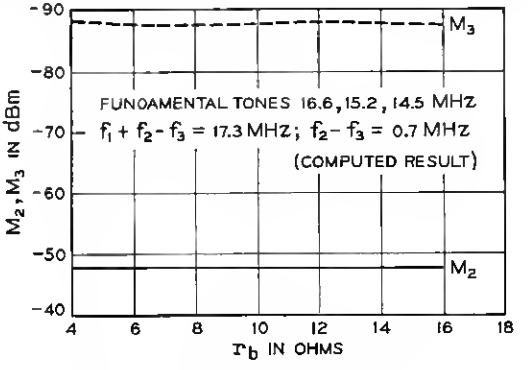

Fig. 14—Variation of M_2, M_3 with r_b.

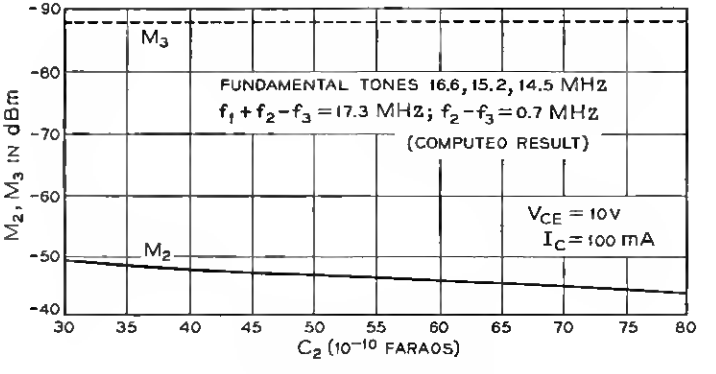

Fig. 15—Variation of M_2, M_3 with C_2.

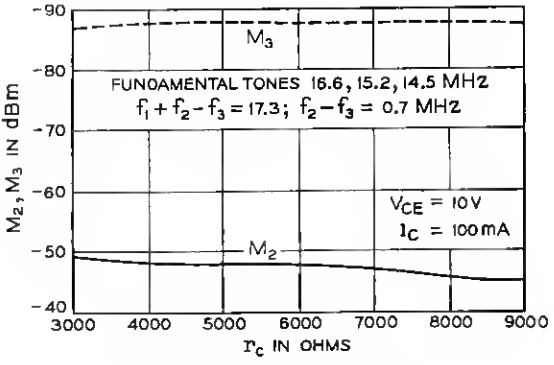

Fig. 16 — Variation of M_2, M_3 with r_e.

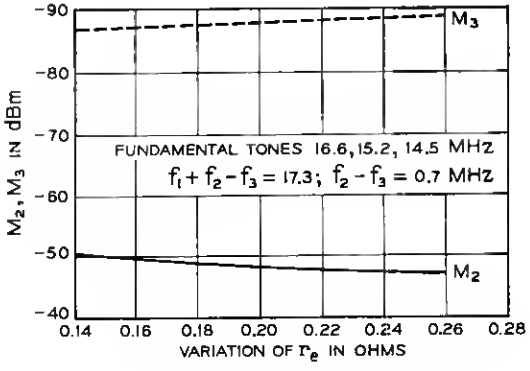

Fig. 17 — Variation of M_2, M_3 with r_e.

of the previous stages cannot be ignored and sometimes the previous stage is dominant. This is especially true if both minimum noise figure (which requires lower bias current) and modulation requirements are to be met by a two stage amplifier. Two analysis tools based on Volterra series are presented bere which enable tbe study of such cascaded stages.

The first approach makes use of the cascaded formulae mentioned earlier; this method illustrates the cascade phenomenon and permits derivation of simple cascade rules.

Consider two cascaded transistors (Fig. 1); let the output voltage (v_2) of the first transistor be denoted by $D(v_g)$; the output voltage (v_3) of the second stage by $E(v_2)$ and $F(v_g)$. Tbe aim is to compute the kernels $F_1(s_1)$, $F_2(s_1, s_2)$, $F_3(s_1, s_2, s_3)$ knowing D and E. To calculate $D(s_1)$, etc., it is necessary to know the load impedance of the first stage which

is the input impedance of the second transistor. This can he computed; thus, for a given generator impedance and hias conditions, $D(s_1)$, $D_2(s_1, s_2)$, $D_3(s_1, s_2, s_3)$ can be determined. $E(s_1)$, $E_2(s_1, s_2)$ and $E_3(s_1, s_2, s_3)$ can he computed for a given load and hias conditions with $R_g = 0$ (voltage v_2 is directly impressed across the second). Now expression v_3 in terms of v_g is given hy

$$v_3 = F(v_g) = E(v_2) = E(D(v_g)) = (E \circ D)(v_g). \tag{30}$$

It is seen that F is related to E and D hy the cascade formulae whose physical significance is discussed helow.

6.1 *Linear Term*

The linear term is given by

$$F_1(s) = D_1(s)E_1(s) \tag{31}$$

which states that the overall gain in dB is the gain of the first stage in dB plus the gain of the last stage in dB.

6.2 *Second Harmonic Term*

The second-degree kernel is given by

$$F_2(s_1, s_2) = E_1(s_1 + s_2)D_2(s_1, s_2) + E_2(s_1, s_2) \prod_{i=1}^{2} D_1(s_i). \tag{32}$$

The first term of the formula states that a given harmonic product from the first transistor $D_2(j\omega_a \pm j\omega_b)$ is amplified hy the second transistor at the harmonic frequency $E_1(j\omega_a \pm j\omega_b)$. The second term shows that the two fundamental tones are amplified hy the first transistor $[D_1(j\omega_a)D_1(\pm j\omega_b)]$ and then the second transistor acts on these tones to produce distortion $E_2(j\omega_a, \pm j\omega_b)$.

Equation (32) is related to the second harmonic distortion (M_2) as follows:

$$M_2 = 20 \log \frac{\sqrt{10^{-3}R_L}}{2} \left| \frac{F_2(s_1, s_2)}{F_1(s_1)F_1(s_2)} \right| \tag{33}$$

$$= 20 \log \frac{\sqrt{10^{-3}R_L}}{2} \left| \left[\frac{D_2(s_1, s_2)}{\prod_{i=1}^{2} D_1(s_i)} \right] \frac{E_1(s_1 + s_2)}{E_1(s_1)E_1(s_2)} + \frac{E_2(s_1, s_2)}{\prod_{i=1}^{2} E_1(s_i)} \right|. \tag{34}$$

The second term is the second harmonic distortion of the last stage. The first term expresses the contribution from the first stage; it approxi-

mately equals

$$\begin{bmatrix}\text{First stage second harmonic}\\ \text{distortion in dBm}\end{bmatrix} - \begin{bmatrix}\text{gain of the last stage}\\ \text{in dB}\end{bmatrix}. \quad (35)$$

This shows that if the gain of the last stage is high, the contribution from the first stage is small. Equation (35) is approximate in two respects; it neglects the frequency effects and the phase addition of the contributions from the first and the second stage. In (35), the second stage gain in question is actually the ratio

$$\frac{E_1(s_1 + s_2)}{E_1(s_1)E_1(s_2)}$$

which involves the two fundamental and the harmonic frequencies. As an example, a shaping network which was introduced increased the gain (18 dB) at the harmonic frequency (0.7) MHz) and decreased the gain at fundamental tones 15.2 MHz (8 dB) and 14.5 MHz (8 dB) with the result the overall distortion was poorer by 34 dB.

6.3 *Third Harmonic Distortion Term*

The third harmonic kernel $F_3(s_1 , s_2 , s_3)$ is given by

$$F_3(s_1 , s_2 , s_3) = E_1(s_1 + s_2 + s_3)D_3(s_1 , s_2 , s_3) + 2E_2(s_1 , s_2 + s_3) \cdot D_1(s_1)D_2(s_2 , s_3) + E_3(s_1 , s_2 , s_3) \prod_{i=1}^{3} D_1(s_i). \quad (36)$$

The first term shows that the third harmonic product of the first stage $[D_3(s_1 , s_2 , s_3)]$ is amplified by the last stage at the harmonic frequency $[E_1(s_1 + s_2 + s_3)]$. The second term is the interaction term; it arises when the second-degree kernel of the last stage $[E_2(s_1 , s_2 + s_3)]$ acts on the sum of the fundamental $[D_1(s_1)]$ and the second harmonic output of the first stage $[D_2(s_2 , s_3)]$. The last term shows that the second stage third-degree kernel $[E_3(s_1 , s_2 , s_3)]$ acts on the fundamental tones amplified at the respective frequencies by the first stage $[D_1(s_1)D_1(s_2)D_1(s_3)]$.

From (36), the overall third harmonic distortion is related to that of the individual transistors by

$$M_3 = 20 \log \frac{1}{4} 10^{-3} R_L \left| \left[\frac{E_1(s_1 + s_2 + s_3)}{\prod_{i=1}^{3} E_1(s_i)} \right] \left[\frac{D_3(s_1 , s_2 , s_3)}{\prod_{i=1}^{3} D_1(s_i)} \right] + 2 \left[\frac{E_2(s_1 , s_2 + s_3)}{\prod_{i=1}^{2} E_1(s_i)} \right] \frac{1}{E_1(s_3)} \left[\frac{D_2(s_2 , s_3)}{\prod_{i=1}^{2} D_1(s_i)} \right] + \left[\frac{E_3(s_1 , s_2 , s_3)}{\prod_{i=1}^{3} E_1(s_i)} \right] \right| . \quad (37)$$

The first term is the contribution from the third harmonic term of the first stage; it is given approximately by

$$\begin{bmatrix}\text{Third harmonic distortion}\\ \text{of the first stage in dBm}\end{bmatrix} - 2\begin{bmatrix}\text{Gain of the last}\\ \text{stage in dB}\end{bmatrix}. \tag{38}$$

The interaction term approximately equals

$$\begin{bmatrix}\text{Second barmonic distortion}\\ \text{of the first stage in dBm}\end{bmatrix} + \begin{bmatrix}\text{Second harmonic distortion}\\ \text{of the second stage in dBm}\end{bmatrix} + 6\text{ dB} - \begin{bmatrix}\text{Gain of the last}\\ \text{stage in dB}\end{bmatrix}. \tag{39}$$

The third term in (37) is the third harmonic distortion of the last stage in dBm.

It is seen that the effect of the first stage and the interaction term can be reduced by increasing the gain of the last stage. Equation (39) illustrates that the second harmonic distortion of each stage should be good. This may become a limitation if the first stage is biased at lower currents.

In the above simplified expressions [(38) and (39)] phase addition and frequency effects have not been considered. In (38), 2 (gain in dB) actually represents

$$20 \log \left| \frac{E_1(j\omega_a \pm j\omega_b \pm j\omega_c)}{E_1(j\omega_a)E_1(\pm j\omega_b)E_1(\pm j\omega_c)} \right|.$$

In (39) the second harmonic distortion is to be measured witb two tones, one at the fundamental and the other at the harmonic frequency

$$\frac{E_2(s_1\ ,\ s_2 + s_3)}{E_1(s_1)E_1(s_2 + s_3)}$$

and then multiplied by the ratio of the gain

$$\frac{E_1(s_2 + s_3)}{E_1(s_1)}.$$

Moreover, the kernel must be made symmetrical by taking the average of three possible combinations.

Thus, the simplified expressions (35), (38), and (39) aro exact if the transistor performance is not frequency dependent; in general, they

can be used to get a qualitative picture. Equations (34) and (37) are indeed exact and take into account the frequency dependence. The computer program is being extended to calculate (34) and (37).

An alternate approach to calculate the distortion of cascaded stages is to analyze the nonlinear equivalent circuit of cascaded transistors using the nodal technique illustrated in Section IV. The nodal equations are derived first; next each nodal voltage is expressed in terms of the Volterra series of the input voltage; tbe resulting vector matrix equations are successively solved. Since the procedure is similar, the details are omitted.

Two common-collector stages were cascaded using this approach. (Fig. 18). The measured values at 120 mA, 10 V with 75 ohm source and load impedances were −87 dBm and −112 dBm for the second and the third harmonic distortion, respectively. The computed distortion values are −88.7 dBm for second and −116.6 dBm for third harmonic distortion. Thus, good agreement with experimental result is obtained.

Tbe cascade formulas are simple, physically meaningful and yield rules of thumb to judge the effect of the first stages. The nodal approach is more complicated. However, the advantage of the nodal approach is that it is general and can be used for an amplifier. For example, a cascade of common-emitter and common-collector stages involves five nodes; if shunt feedback is used at the input and at the output, the same program can be used to analyze this amplifier. (Cascade formulas do not take feedback into account.) In general, the nodal approacb can be extended to study frequency-dependent nonlinear network with n nodes, if the nonlinearities are small.

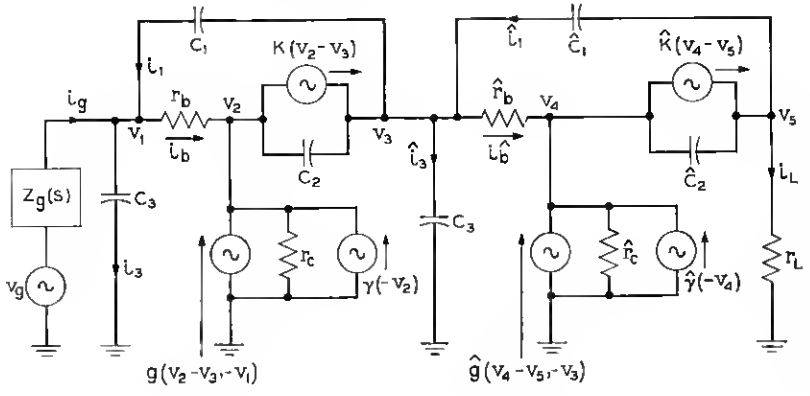

Fig. 18 — Common-collector — common-collector nonlinear equivalent circuit.

VII. ENGINEERING APPLICATIONS

A few pertinent practical applications of the work are described below. These results were either first predicted by the model and tben verified in the laboratory or first experimentally observed and then confirmed by analysis.

In the initial design of L4 repeater a common-emitter—common-emitter—common-collector configuration[28] was used in the power amplifier. The third harmonic modulation performance was not as good as desired. This led first to the study of tbe output common-collector stage. As shown in Fig. 19, the increase in source impedance increases the distortion of the common-collector stage. Since the preceding common-emitter stage output impedance is high, the common-collector performance was not optimum. Secondly, the preceding common-emitter stage was studied because the gain of the common-collector stage is low. (see Section VI) As shown in Fig. 20, increase in load impedance beyond optimum R_L degrades its performance radically. Since the common-collector input impedance is high, the common-emitter stage performance was not optimum eitber. Thus, in the redesign work by Ken Tantarelli, tbe common-collector output stage is not being used.

Another interesting application feature was the improvement in modulation performance of the common-emitter stage with increase in voltage. As shown in Fig. 8, it is a function of load impedance, and at about 150Ω, maximum improvement was obtained.

New coaxial systems are currently being studied to operate at higher frequencies. Different configurations have been examined for the output stage. The model showed that common-collector and common-base performance is poorer with an increase in frequency and thus the use of these stages as output stages was questioned (unless transistors with

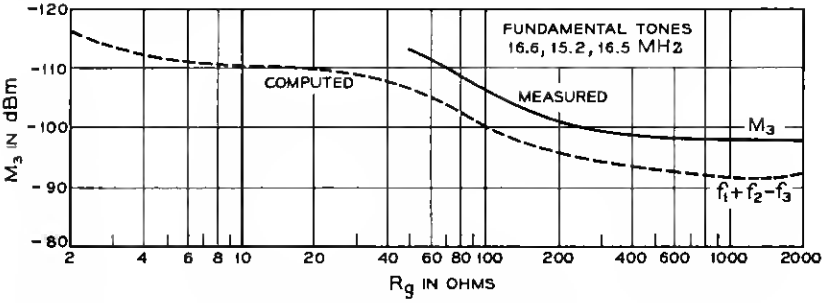

Fig. 19—Common-collector; M_3 variation with source impedance; $I_c = 120$ mA; $V_{cc} = 10V$; $R_L = 75\ \Omega$.

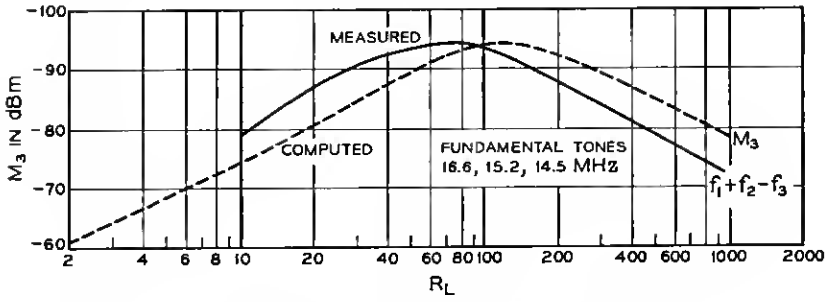

Fig. 20—Common-emitter; M_3 variation with load impedance; I_c = 120 mA; V_{ce} = 10V; R_g = 75 Ω.

higher f_t's are available). Recently when a new, high-frequency modulation test set was built, experiments confirmed the prediction. The third harmonic coefficient ($M3$) for $a + b - c$ product was 8 dB poorer at 36.5 MHz (due to signals at 36.5 MHz, 40.1 MHz, and 43.1 MHz) compared to the value at 17.3 MHz (due to signals at 14.5, 15.2, and 16.6 MHz). The common-emitter configuration modulation performance suffered only about one dB degradation.

VIII. CONCLUSION AND ACKNOWLEDGMENT

This paper has presented a useful analysis tool for investigating the frequency-dependent nonlinear behavior of transistors. A digital program for all the three configurations has been prepared. The results obtained compare favorably with experimental results. The closed-form expressions yield a qualitative picture of distortion. The Volterra series proves useful in examining cascaded transistors; a few rules of thumb are derived and a general nodal analysis which can be extended to cascaded stages with feedback is developed. The practical applications cited show that the technique can be useful in the computer-aided optimal design of linear transistor feedback amplifiers.

The author acknowledges gratefully the cooperation he received from Lee C. Thomas who is responsible for much of the initial development of the model; he has been particularly concerned about the cancellation mechanism which he observed in the analog computer simulation. The author wishes to thank Mr. Jack Huang, who first suggested the model, Miss J. A. Nicosia, who wrote the program, Mr. F. Kelcourse for many useful discussions, and Mr. R. E. Maurer for reading the draft. The author would also like to thank Dr. F. H. Blecher for his encouragement and continued interest and guidance.

APPENDIX A

A.1 *Higher-Dimensional Transforms*

The second-degree case is illustrated as an example. From (4),

$$y_2(t) = \int_0^t \int_0^t c_2(t - \tau_1 , t - \tau_2) \prod_{i=1}^{2} x(\tau_i)\, d\tau_i . \tag{40}$$

If the system is physically realizable, $c_2(t - \tau_1 , t - \tau_2) = 0$, for $\tau_i > t$. Hence, the limits can be extended to ∞.

$$y_2(t) = \int_0^\infty \int_0^\infty c_2(t - \tau_1 , t - \tau_2) \prod_{i=1}^{2} x(\tau_i)\, d\tau_i . \tag{41}$$

Introducing dummy variables t_1 and t_2, the two-dimensional transform is taken

$$\begin{aligned} Y_2(s_1 , s_2) &= \int_0^\infty \int_0^\infty y_2(t_1 , t_2) \exp(-s_1 t_1) \exp(-s_2 t_2)\, dt_1\, dt_2 \\ &= \int_0^\infty dt_1 \int_0^\infty dt_2 \left[\int_0^\infty d\tau_1 \int_0^\infty d\tau_2\, c_2(t_1 - \tau_1 , t_2 - \tau_2) \right. \\ &\qquad \left. \cdot \prod_{i=1}^{2} x(\tau_i)\, d\tau_i \right] \exp(-s_1 t_1) \exp(-s_2 t_2). \end{aligned} \tag{42}$$

Substituting $t_1 - \tau_1 = m_1$, $t_2 - \tau_2 = m_2$, and using the fact that $c_2(m_1 , m_2) = 0$ for $m_i < 0$ yields

$$\begin{aligned} Y_2(s_1 , s_2) &= \int_0^\infty dm_1 \int_0^\infty dm_2 \int_0^\infty d\tau_1 \int_0^\infty d\tau_2\, c_2(m_1 , m_2) x(\tau_i) x(\tau_2). \\ &\qquad \cdot \exp(-s_1 m_1) \exp(-s_1 \tau_1) \exp(-s_2 m_2) \exp(-s_2 \tau_2) \qquad (43) \\ &= C_2(s_1 , s_2)\, X(s_1)\, X(s_2). \qquad (44) \end{aligned}$$

A.2 *The Output of the Kernels to Sinusoidal Inputs*

For the second-degree case, consider two sinusoidal signals at frequencies f_a and f_b. The input $x(\tau)$ equals,

$$x(\tau) = \left[\frac{\exp(j\omega_a \tau) + \exp(-j\omega_a \tau)}{2} \right] + \left[\frac{\exp(j\omega_b \tau) + \exp(-j\omega_b \tau)}{2} \right]. \tag{45}$$

From (41)

$$y(t) = \int_0^\infty d\tau_1 \int_0^\infty d\tau_2\, c_2(t - \tau_1 , t - \tau_2)$$

$$\cdot\left[\frac{\exp(j\omega_a\tau_1) + \exp(-j\omega_a\tau_1)}{2} + \frac{\exp(j\omega_b\tau_1) + \exp(-j\omega_b\tau_1)}{2}\right]$$

$$\cdot\left[\frac{\exp(j\omega_a\tau_2) + \exp(-j\omega_a\tau_2)}{2} + \frac{\exp(j\omega_b\tau_2) + \exp(-j\omega_b\tau_2)}{2}\right]. \quad (46)$$

Considering one cross term only,

$$\int_0^\infty d\tau_1 \int_0^\infty d\tau_2\, c_2(t - \tau_1 , t - \tau_2)$$

$$\cdot\tfrac{1}{4}\exp(j\omega_a\tau_1)\exp(j\omega_b\tau_2). \quad (47)$$

Substituting $m_1 = t - \tau_1$, $m_2 = t - \tau_2$ and carrying out the integration yields

$$\tfrac{1}{4}C_2(j\omega_a ; j\omega_b)\exp[j(\omega_a + \omega_b)t]. \quad (48)$$

This term occurs twice as does its complex conjugate.

Hence, the output due to the $a + b$ term alone is

$$y_{a+b}(t) = |C_2(j\omega_a , j\omega_b)| \cos[(\omega_a + \omega_b)t + \varphi_{a+b}]. \quad (49)$$

The $2\omega_a$ term and its conjugate occur only once in (46); hence, it is 6 dh better. The response of the third harmonic kernel to three sinusoidal inputs is similarly treated.

A.3 *Cascade Relations*

For the system shown in Fig. 1, the cascade formula are given below. The cascade relations can be symbolically written as

$$Z = F(x) = E(y) = E(D[x]) = (E\ o\ D)(x). \quad (50)$$

The formula are

$$F_1(s_1) = E_1(s_1)D_1(s_1) \quad (51)$$

$$F_2(s_1 , s_2) = E_1(s_1 + s_2)D_2(s_1 , s_2) + E_2(s_1 , s_2)\prod_{i=1}^{2} D_1(s_1) \quad (52)$$

$$F_3(s_1 , s_2 , s_3) = E_1(s_1 + s_2 + s_3)D_3(s_1 , s_2 , s_3)$$

$$+ 2E_2(s_1 , s_2 + s_3)D_1(s_1)D_2(s_2 , s_3) + E_3(s_1 , s_2 , s_3)\prod_{i=1}^{3} D_1(s_i). \quad (53)$$

A physical interpretation of the formula for cascaded transistors is given in Section VI. The procedure for deriving the cascade relation is as follows: the output $Z(t)$ of the last stage is expressed in terms of the Volterra series of its input. (Only two terms are considered)

$$Z(t) = \int_0^\infty e_1(t - \tau_1)y(\tau_1)\,d\tau_1 + \int_0^\infty \int_0^\infty e_2(t - \tau_1 , t - \tau_2) \prod_{i=1}^{2} y(\tau_i)\,d\tau_i . \quad (54)$$

The output of the first stage $y(t)$ is related to its input by

$$y(\tau) = \int_0^\infty d_1(\tau - \sigma_1)x(\sigma_1)\,d\sigma + \int_0^\infty \int_0^\infty d_2(\tau - \sigma_1 , \tau - \sigma_2) \prod_{i=1}^{2} x(\sigma_i)\,d\sigma_i \quad (55)$$

Substituting (55) in (54), terms of the same degree are collected; as an example, the first second-degree term equals

$$\int d\tau\, e_1(t - \tau) \iint d_2(\tau - \sigma_1 , t - \sigma_2) \prod_{i=1}^{2} x(\sigma_i)\,d\sigma_i . \quad (56)$$

Taking the two-dimensional transforms yields

$$E_1(s_1 + s_2)D_2(s_1 , s_2) \prod_{i=1}^{2} X(s_i). \quad (57)$$

APPENDIX B

The Nonlinear Parameters

From (15),

$$I_c = f(I_E)h(V_{CB}). \quad (58)$$

A two-dimensional Taylor's series expansion of (58) is taken; i_c is expressed by $K(v_2)$ and $v_{CB} = v_3 - v_1$. Hence,

$$i_c = g(v_2 , v_3 - v_1) = g_1(v_2 , v_3 - v_1) + g_2(v_2 , v_3 - v_1) + g_3(v_2 , v_3 - v_1), \quad (59)$$

where

$$g_1(v_2 , v_3 - v_1) = \alpha_1\hat{M}_0K_1v_2 + \hat{M}_1(v_3 - v_1), \quad (60)$$

$$g_2(v_2 , v_3 - v_1) = \alpha_2\hat{M}_0K_1^2(v_2)^2 + m_2(v_3 - v_1)^2 + \alpha_1\hat{M}_0K_2(v_2)^2 + \alpha_1\hat{M}_1K_1(v_2)(v_3 - v_1), \quad (61)$$

and

$$g_3(v_2 , v_3 - v_1) = \alpha_3\hat{M}_0(K_1)^3(v_2)^3 + m_3(v_3 - v_1)^3 + \alpha_1\hat{M}_2K_1v_2(v_3 - v_1)^2 + \alpha_2\hat{M}_1K_1^2v_2^2(v_3 - v_1) + \alpha_1\hat{M}_0K_3(v_2)^3 + 2\alpha_2\hat{M}_0K_1K_2(v_2)^3 + \alpha_1\hat{M}_1K_2(v_2)^2(v_3 - v_1). \quad (62)$$

The avalanche coefficients are given below.

$$\hat{M}_0 = \frac{1}{1 - \left(\frac{V_{CB}}{V_{CBO}}\right)^n} \tag{63}$$

$$\hat{M}_1 = (\hat{M}_0)' = \frac{n(V_{CB})^{n-1}}{(V_{CBO})^n} (\hat{M}_0)^2 \tag{64}$$

$$\hat{M}_2 = \tfrac{1}{2}(\hat{M}_1)' = \tfrac{1}{2}(n-1)\frac{\hat{M}_1}{V_{CB}} + \frac{(\hat{M}_1)^2}{\hat{M}_0} \tag{65}$$

$$\hat{M}_3 = \tfrac{1}{3}(\hat{M}_2)' = \tfrac{2}{3}\hat{M}_2\left(\frac{(n-1)}{2V_{CB}} + \frac{2\hat{M}_1}{\hat{M}_0}\right) - \frac{\hat{M}_1}{3}\left[\frac{(n-1)}{2(V_{CB})^2} + \left(\frac{\hat{M}_1}{\hat{M}_0}\right)^2\right]. \tag{66}$$

The coefficients m_1, m_2, and m_3 equal $m_i = I_C(\hat{M}_i/\hat{M}_0)$; $i = 1, 2, 3$, where I_C is the collector dc bias current.

The h_{FE} coefficients are given below:

$$\alpha_1 = \frac{h_{FE\,\max}}{h_{FE\,\max} + 1 + a\log^2\frac{I_C}{I_{C\,\max}} + 2a\log e\log\frac{I_C}{I_{C\,\max}}} \tag{67}$$

$$\alpha_2 = -\frac{1}{2I_C}\frac{(\alpha_1)^3}{h_{FE\,\max}}\,2a\log e\left[\log\frac{I_C}{I_{C\,\max}} + \log e\right] \tag{68}$$

$$\alpha_3 = \frac{\alpha_1}{6}\left[\frac{-2\alpha_2}{I_C} + 12\frac{(\alpha_2)^2}{(\alpha_1)^2} - \frac{1}{(I_C)^2}\frac{(\alpha_1)^3}{h_{FE\,\max}}\,2a(\log e)^2\right]. \tag{69}$$

The collector capacitance coefficients are given by

$$\gamma_1 = k(V_{CB})^{-\frac{1}{3}} \tag{70}$$

$$\gamma_2 = \frac{-1}{6}k(V_{CB})^{-\frac{4}{3}} \tag{71}$$

$$\gamma_3 = \frac{k}{27}(V_{CB})^{-\frac{7}{3}}. \tag{72}$$

From (62) for $g_3(v_2\,;\, v_3 - v_1)$, $\hat{g}_3$ is obtained by replacing $B_1(s_i)$ for v_2 and $C_1(s_i) - A_1(s_i)$ for $(v_3 - v_1)$; moreover, the kernel must also be symmetrical. Since the procedure is the same as for $\hat{g}_2$ it is omitted. The interaction terms are given below:

$$\begin{aligned}\hat{g}_{23} &= 2\alpha_2\hat{M}_0K_1^2\,\overline{B_1(s_1)B_2(s_2\,,\,s_3)} \\ &+ 2m_2\,\overline{[C_1(s_1) - A_1(s_1)][C_2(s_2\,,\,s_3) - A_2(s_2\,,\,s_3)]} \\ &+ \alpha_1\hat{M}_1K_1\,\overline{B_2(s_1\,,\,s_2)[C_1(s_3) - A_1(s_3)]}\end{aligned}$$

$$+ \alpha_1 \hat{M}_1 K_1 \overline{B_1(s_1)[C_2(s_2, s_3) - A_2(s_2, s_3)]} \tag{73}$$

$$\hat{\gamma}_{23} = 2\gamma_2 \overline{[C_1(s_1) - B_1(s_1)][C_2(s_2, s_3) - B_2(s_2, s_3)]} \tag{74}$$

where $-$ denotes symmetrical kernel.

APPENDIX C

A2436 is an n-p-n silicon transistor with overlay type of construction. Its f_T ranges from 800 to 1000 MHz. It is a power transistor with current capability of 1 amp and can handle 2.2 watts of power.

Typical parameter values for transistor type 2436 27 at 120 mA, 10V are given below:

I_c = 0.12 amps.
r_b = 13.6 ohms
r_e = 5200 ohms
C_1 = $(6)10^{-12}$ farads
C_2 = $(3.97)10^{-9}$ farads
C_3 = $(9.2)10^{-12}$ farads
Z_g = 50 ohms
Z_L = 50 ohms
V_{CB} = 10 volts
V_{CBO} = 350 volts
n = 2
re_1 = 0.2165 ohms
a = 0.38
$h_{FE\ max}$ = 122
$I_{C\ max}$ = 0.633 amps.

REFERENCES

1. Lotsch, H., Third Order Distortion and Cross-Modulation in a Grounded Emitter Transistor Amplifier, IRE Trans. Audio, March, 1961, pp. 49–56.
2. Mallinckrodt, A. J. and Gardner, F. M., Distortion in Transistor Amplifiers, IRE Trans. Electron Devices, July, 1963, pp. 288–289.
3. Krislov, Y. D., Nonlinear and Cross-Modulation Distortion in Transistor Amplifiers, Telecommun. Radio Eng., March, 1965, pp. 97–103.
4. Lotsch, H., Survey of Nonlinear Distortions in Transistor Stages Including Cross-Modulation, Arch. Ebek Vebertragung 14, No. 5, 1960, pp. 204–216.
5. Reynolds, J., Nonlinear Distortions and Their Cancellation in Transistors, IEEE Electron Devices, November, 1965.
6. Riva, G. M., Beneteau, P. J., and DallaVolta, E., Amplitude Distortion in Transistor Amplifier, Proc. IEEE, No. 3, March, 1964, pp. 481–490.
7. Meyer, N. I., Nonlinear Distortion in Transistor Class A Amplifiers at Low and Medium Frequencies, Proc. IEEE, May, 1959, pp. 481–489.
8. Meyer, N. I., On the Variation of Transistor Small Signal Parameters with Emitter Current and Collector Voltage, J. Electron. Control, 4, 1958, p. 305.

9. Meyer, N. I., *Nonlinear Distortion and Small Signal Parameters of Alloyed Junction Transistors,* Danish Science Press Ltd., Copenhagen, 1960.
10. Thomas, L. C., Broadband linearization of Transistor Amplifiers, Presented at International Solid State Circuits Conference, February, 1967.
11. Narayanan, S., Transistor Distortion Analysis Using Volterra Series Representation, (Oral presentation at International Conference on Communications, June, 1967).
12. Volterra, V., *Theory of Functionals and of Integral and Integrodifferential Equations,* Dover Publications, New York, 1959.
13. Wiener, N., Response of a Nonlinear Device to Noise, MIT, Radiation Laboratory, Cambridge, Mass., Report No. 129, (V-16), April, 1942.
14. Bose, A. G., A Theory of Nonlinear Systems, Technical Report 309, Research Laboratory of Electronics, MIT, May 15, 1956.
15. Wiener, N., *Nonlinear Problems in Random Theory,* MIT Press, Cambridge, Mass., 1958.
16. Brilliant, M. B., Theory of the Analysis of Nonlinear Systems, Technical Report 345, Research Laboratory of Electronics, MIT, March 3, 1958.
17. George, D. A., Continuous Nonlinear Systems, Technical Report 355, Research Lab of Electronics, MIT, July 22, 1959.
18. Cbesler, D. A., Nonlinear Systems with Gaussian Inputs, Technical Report 366, Research Lab of Electronics, MIT, February 15, 1960.
19. Barrett, J. F., The Use of Functionals in tbe Analysis of Nonlinear Physical Systems, Statistical Advisory Unit, Report No. 1/57, Ministry of Supply, Great Britain, 1957.
20. VanTrees, H. L., *Volterra Series Representation of Optimum Nonlinear Control Systems,* MIT Press, Cambridge, Mass., 1962.
21. VanTrees, H. L., Functional Techniques for the Analysis of the Nonlinear Behavior of Phase-Locked Loops, Proc. IEEE, *52,* No. 8, August, 1964, pp. 894–911.
22. Alper, P., A Consideration of Discrete Volterra Series, 1965, Joint Automatic Control Conference, Rensselaer Polytecbnic Institute, Troy, N. Y., June, 1965, p. 96.
23. Bush, A. M., Some Techniques for the Synthesis of Nonlinear Systems, Sc-D Thesis, Dept. of Electrical Engineering, MIT, Cambridge, Mass., May, 1965.
24. Narayanan, S., Transform Methods for Special Nonlinear Systems, Ph.D. Thesis, Carnegie Tech., Pittsburgh, Pa., May, 1965.
25. Flake, R. H., Volterra Series Representation of Time-Varying Nonlinear Systems, Proc. Second International Congress of IFAC on Automatic Control Based, Switzerland, Paper No. 408/1, 1963.
26. Ku, Y. H. and Wolf, A. A., Volterra-Wiener Functionals for the Analysis for Nonlinear Systems, J. Franklin Inst., *281,* No. 1, January, 1966, pp. 9–26.
27. Phillips, A. B., *Transistor Engineering,* McGraw-Hill Book Co., New York, 1962.
28. Kelcourse, F. C. and Labbe, L. P., Transistor Feedback Amplifiers for 0.5 m/c-20 m/c Long Haul Coaxial Cable Transmission System, IEEE NEREM Conference, 1964.